

Journal of Semiconductors

JOS

iopscience.iop.org/jos
www.jos.ac.cn

Synthesis and characterization of ZnS-based quantum dots to trace low concentration of ammonia

Uma Devi Godavarti, P. Nagaraju, Vijayakumar Yelsani, Yamuna Pushukuri, P. S. Reddy, and Madhavaprasad Dasari

Citation: U D Godavarti, P. Nagaraju, V Yelsani, Y M N P S K ri, P. S. Reddy, and M Dasari, Synthesis and characterization of ZnS-based quantum dots to trace low concentration of ammonia[J]. *J. Semicond.*, 2021, In Press .

View online: <http://www.jos.ac.cn/article/shaid/46ccc881387dd9957d8385db32f185da7271ddb72aa67a8e578101d7dd585613>

Articles you may be interested in

[High performance GaN-based hybrid white micro-LEDs integrated with quantum-dots](#)

Journal of Semiconductors. 2020, 41(3), 032301 <https://doi.org/10.1088/1674-4926/41/3/032301>

[Light-emitting diodes based on colloidal silicon quantum dots](#)

Journal of Semiconductors. 2018, 39(6), 061008 <https://doi.org/10.1088/1674-4926/39/6/061008>

[Quantum light source devices of In\(Ga\)As semiconductor self-assembled quantum dots](#)

Journal of Semiconductors. 2019, 40(7), 071902 <https://doi.org/10.1088/1674-4926/40/7/071902>

[Research on the photoluminescence of spectral broadening by rapid thermal annealing on InAs/GaAs quantum dots](#)

Journal of Semiconductors. 2020, 41(12), 122101 <https://doi.org/10.1088/1674-4926/41/12/122101>

[Three-dimensional hierarchical CuO gas sensor modified by Au nanoparticles](#)

Journal of Semiconductors. 2019, 40(2), 022101 <https://doi.org/10.1088/1674-4926/40/2/022101>

[Recent progress on gas sensors based on graphene-like 2D/2D nanocomposites](#)

Journal of Semiconductors. 2019, 40(11), 111608 <https://doi.org/10.1088/1674-4926/40/11/111608>



Follow JOS WeChat public account for more information

Synthesis and characterization of ZnS-based quantum dots to trace low concentration of ammonia

Uma Devi Godavarti¹, P. Nagaraju^{1, †}, Vijayakumar Yelsani², Yamuna Pushukuri³, P. S. Reddy⁴, and Madhavaprasad Dasari⁵

¹Nanosensor Research Laboratory, Department of Physics, CMR Technical Campus, Medchal, Hyderabad – 501 401, Telangana, India

²Department of Physics, Anurag University, Hyderabad, Telangana, India

³Department of Physics, Mallareddy Engineering College (Autonomous), Dulapally, Hyderabad, India

⁴Department of Applied Sciences, NIT Goa, Goa, India

⁵Department of Physics, Gitam University, Visakhapatnam (A. P.), India

Abstract: In the present work, a solution-based co-precipitation method has been adopted to synthesize pure and cobalt-doped ZnS quantum dots and characterized by XRD, SEM, TEM with EDX, FTIR and gas sensing properties. XRD analysis has shown a single phase of ZnS quantum dots having a zinc blend structure. TEM and XRD line broadening indicated that the average crystallite size in the sample is in the range of 2 to 5 nm. SEM micrographs show spherical-shaped quantum dots. FTIR studies show that cobalt has been successfully doped into the ZnS cubic lattice. EDX spectra have analyzed the elemental presence in the samples and it is evident that the spectra confirmed the presence of cobalt (Co), zinc (Zn), oxygen (O), and sulphur (S) elements only and no other impurities are observed. The ZnS-based quantum dot sensors reveal high sensitivity towards 50 ppm of ammonia vapors at an operating temperature of 70 °C. Hence, ZnS-based quantum dots can be a promising and quick traceable sensor towards ammonia sensing applications with good response and recovery times.

Key words: ZnS; co-precipitation; cobalt doped ZnS; XRD; quantum dots; gas sensor; ammonia; response

Citation: U D Godavarti, P. Nagaraju, V Yelsani, Y M N P S K ri, P. S. Reddy, and M Dasari, Synthesis and characterization of ZnS-based quantum dots to trace low concentration of ammonia[J]. *J. Semicond.*, 2021, in press

1. Introduction

Semiconductor nanomaterials referred to as quantum dots (QDs) have been extensively popular in the recent past due to their distinctive size-dependent optical properties, tailored surface modification and good biocompatibility leading to use as sensor element for many industrial and agricultural applications. As the particle size is reduced to smaller than their exciton Bohr radius, the excitons formed are confined to a potential well. Relatively, changes exist in the fundamental properties of semiconducting materials exist like an increased band gap, reduced melting point, electronic orbitals density and geometries of bonding by simply decreasing particle size. These size-controlling properties affect a semiconductor material instantly restricting to a nanometer scale in all three dimensions, leading to the semiconducting spherical nanocrystals, also referred as quantum dots (QDs)^[1]. In addition, quantum dots referred as those whose particle size is less than 100 nm. Nowadays, QDs are fabricated by incorporating elements of the II–VI group that have been acquiring scientific attraction due to their distinct properties.

Among all the semiconducting materials, ZnS is the cutting-edge material that can be preferred as the perfect alternative in gas sensors. It has a large surface to volume (s/v) ratio, high Bohr exciton radius and huge exciton binding energy,

wide bandgap and quantum confinement effect. The exceptionality of these materials is tailoring the electronic properties by doping with suitable metals and through the impact of the carrier's confinement. ZnS, an II–VI semiconductor, non-toxic, has a wide bandgap of 3.68 eV (for bulk) that realizes a good host for the total number of transition and rare earth metal ion dopants contribute to significant optical and magnetic properties. These materials are very useful in designing short-wavelength LEDs, electroluminescence devices, sensors, laser diodes, flat panel display, biological imaging, solar cells, optoelectronic devices and labelling^[2–7]. There are numerous approaches to fabricate nanoparticles (quantum dots), such as the aqueous method^[8], chemical bath deposition^[9,10], refluxing technique^[11], pulsed laser ablation^[12], solid-state reaction method^[13], solvothermal technique^[14], hydrothermal method^[15,16], co-precipitation and colloidal thermolysis and aerosol assisted chemical vapor deposition^[17–22]. Among all these approaches, co-precipitation is the uncomplicated and cost-efficient method. In this technique, various parameters such as pH, temperature and time of reaction, initial solution concentration and material are chosen, which play a crucial role in preparing ceramic powders with the required shape and size.

Nowadays, in the atmosphere, ammonia is being released to a large extent multiplied by human activity. When a large extent of nitrification process is done to the agricultural land in the form of fertilizer (NH₃), then due to run-off from the land it leads to acidification of water bodies that endangers aquatic organisms. Similarly, excessive nutrients in

Correspondence to: P. Nagaraju, nagarajuphysics@gmail.com

Received 16 APRIL 2021; Revised 17 JUNE 2021.

©2021 Chinese Institute of Electronics

lakes or water bodies lead to eutrophication. The total worldwide contribution of nitrogen fixation related to ammonia emission approaches 1.0 Tg/year^[23]. Furthermore, many chemical industries produce ammonia for the manufacture of fertilizers and utilize it in refrigeration systems. But this exposure to higher concentrations of ammonia leads to severe health hazards. Near intensive farming also high concentration levels than the allowed exposure limit result in unhealthy conditions inside the stables for farmers and animals, wherever the concentration levels are the maximum^[24]. Its odour can detect the high concentration of ammonia, but it is necessary to detect the low gas concentration, yet the human nose fails to detect it. Hence it is essential to design a sensor to detect low concentrations of ammonia vapors.

In the present investigations, ZnS-based quantum dots were synthesized using the co-precipitate technique to detect the low concentration of ammonia. To improve gas sensing properties, divalent cobalt ions with different at.% were doped into the ZnS system. The ionic radius of the cobalt with 0.058 nm is in close proximity to that of the 0.06 nm ionic radius of Zn²⁺ divalent cation. Hence, divalent Co²⁺ transition metal ion can be successfully incorporated in the ZnS quantum dots up to a particular absorbance of 0.05 – 0.25 at.%. Thus, we have synthesized ZnS based quantum dots with cobalt as dopant with 0.05 at.% and 0.25 at.%. Synthesized pure ZnS quantum dots, cobalt doped ZnS quantum dots were systematically studied their structural, morphological and chemical properties. With the aid of these properties, it is demonstrated that the dopant cobalt is embedded in the ZnS quantum dots. Gas sensing properties of these quantum dots were performed towards 50 ppm of ammonia vapors at an operating temperature of 70 °C in static mode and the results were reported.

2. Materials and Methods

2.1. Materials

All the reagents used in the present study are analytical grade (99%) without any further purification procured from Sigma Aldrich, India.

2.2. Experimental studies

Pure and cobalt-doped ZnS (Zn_{1-x}Co_xS with $x = 0.00, 0.05, \text{ and } 0.25$ at.%) powdered samples were synthesized by the co-precipitation method. Raw materials required for the synthesis of pure ZnS are zinc acetate dihydrate [Zn(CH₃COO)₂·2H₂O] of 1 M dissolved in distilled water (50 mL) and another sodium sulfide [Na₂S] of 1 M is dissolved in distilled water (50 mL) separately and then both the solutions were combined after continuous magnetic stirring for 2h to obtain the pH of 13.5. Precipitate in white color was obtained, which was then separated by using centrifugation. The separation of precipitate is done after washing the prepared sample with distilled water and ethanol several times. It is then dried under vacuum conditions at 600 °C to get powder samples of ZnS quantum dots. Once the pure ZnS sample is obtained, then for the synthesis of cobalt incorporated ZnS quantum dots, zinc acetate and cobalt acetate were taken as starting precursors. These precursors were dissolved in deionized water separately and mixed. Later on, to obtain the pH 13.5, sodium sulfide is added dropwise and stirred for

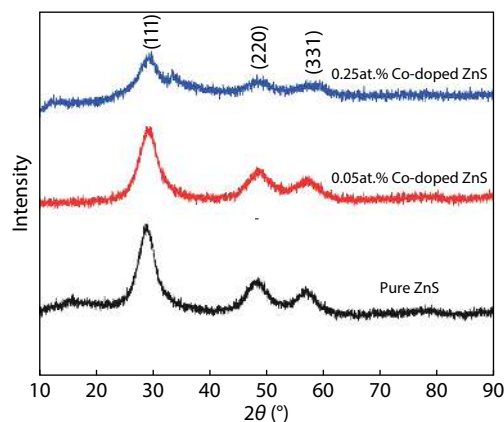


Fig. 1. X-ray diffraction pattern of ZnS and cobalt-doped ZnS quantum dots.

2 h. The precipitate thus obtained is then drained and then for the removal of all sodium particles, the residue was washed with ethanol several times. At the end of this procedure, the wet precipitate has dried to obtain cobalt-doped quantum dots.

2.3. Characterization

The prepared samples were analyzed by X-ray powder diffraction (XRD) using XPERT-PRO (Model: PW-3710) operated at 45 kV with 40 mA with a Cu-K_α radiation source of wavelength 0.154 nm in the range of 10°–90° of Bragg's angle to determine the structural parameters. A scanning electron microscope (SEM) (Model: JSM6100) with an image analyzer was used to analyze the morphological features of the pure and cobalt-doped ZnS quantum dots. Transmission electron microscopy (TEM) was performed using a Hitachi (Model: H-7500) with an operating voltage of 200 kV. A Fourier transform infrared spectroscopy study was carried out to determine the chemical composition of the samples using Thermo Nicolet Nexus 670.

2.4. Gas sensing characterization

The gas sensing characterizations have been performed using an indigenous air sealed gas testing chamber in the static method using a Keithley electrometer (6517B). The required Ohmic electrical contacts were established on the sensor element with the help of thin copper wires and highly conducting silver electrodes. This paper ought to report the gas sensing properties of ZnS and cobalt-doped ZnS quantum dots at an operating temperature of 70 °C towards 50 ppm of ammonia.

3. Results and discussion

3.1. Structural studies

From X-ray diffraction, as shown in Fig. 1, it is noticed that there are three major diffraction peaks for ZnS and cobalt-doped ZnS quantum dots related to (111), (220) and (311) planes which are analyzed to coincide with the standard JCPDS card No. 05-0566 confirming the cubic ZnS structure. For cobalt-doped ZnS, the diminished intensities of diffraction peaks were observed, which imply that Co²⁺ ions are incorporated effectively in the inner lattice of Zn²⁺ ions of ZnS lattice. It is also noticed either no extra or any impurity phases evident in cobalt-doped ZnS samples, indicating

Table 1. Structural properties of pure and cobalt-doped ZnS quantum dots.

| Sample | Lattice constant 'a' (nm) | Volume of unit cell (10^{-30}) m ³ | Crystallite size D (nm) | Strain (ϵ) (10^{-4}) |
|----------------------------|---------------------------|---|-------------------------|-------------------------------------|
| ZnS | 0.529 | 148.03 | 4.84 | 2.76 |
| 0.05 at.% cobalt doped ZnS | 0.527 | 146.36 | 2.43 | 4.23 |
| 0.25 at.% cobalt doped ZnS | 0.524 | 143.88 | 2.81 | 4.87 |

that the prepared samples are single in phase, thereby clearly indicating that cobalt has been incorporated into the lattice a substitution atom. Applying the subsequent relation, the lattice constant 'a' was computed using the following equation^[25],

$$d_{hkl} = \frac{a}{\sqrt{h^2 + k^2 + l^2}},$$

where d is interatomic distance, a is lattice constant and h , k , l are Miller indices. The calculated lattice parameters of the samples are tabulated in Table 1. For cobalt-doped ZnS quantum dots there is a simultaneous decrement in the lattice parameter is observed. Since the Co^{2+} ions that are incorporated into the Zn^{2+} ions of ZnS lattice, the ionic radii of Co^{2+} being 0.058 nm which is nearly the same as that of Zn^{2+} ions 0.060 nm^[26, 27], which is in agreement with the previously reported work by Salem *et al.* and Poornaprakash *et al.*^[28, 29]. Due to this reason, the parameters of the unit cell do not vary notably with the increasing doping concentration of cobalt. From the obtained results, the volume of the unit cell can be estimated using the lattice parameter a . According to Vegard's law, the unit cell volume also decreases with the dopant concentration^[30, 31], as shown in Table 1. Using Scherrer's formula, the average crystallite size (D) was determined with the following relation^[32],

$$D = \frac{0.9\lambda}{\beta \cos\theta},$$

where λ is the wavelength of X-rays, θ is diffraction angle and β is full-width half maxima (FWHM). With the increasing of cobalt doping concentration in the ZnS matrix, the diminishing values of D is observed, which is in the range of 2 to 5 nm, which are also called quantum dots since the synthesized nanoparticles are in the quantum regime as its size is less than exciton Bohr radius^[33]. Compared with the pure ZnS quantum dots, the crystallite size of the 0.05 at.% cobalt doped ZnS quantum dots is reduced due to distortion and micro-strain induced in the lattice due to the incorporation of cobalt ions in the ZnS lattice^[34]. The slight increase in the crystallite size in the case of 0.25 at.% of cobalt-doped ZnS quantum dots is due to the enhancement of grain surface growth due to the excess concentration of cobalt. The calculated average crystallite size values are tabulated in Table 1.

The micro strain was determined using the following equation^[35],

$$\epsilon = \frac{\beta}{4\tan\theta}$$

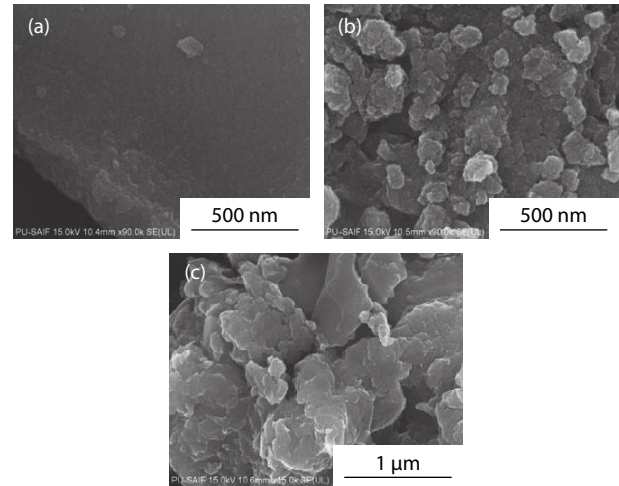


Fig. 2. SEM images of (a) ZnS (b) 0.05 at.% cobalt doped ZnS quantum dots (c) 0.25 at.% cobalt doped ZnS quantum dots.

In strain values as depicted in Table 1, we have noticed a sudden rise in the strain from pure ZnS to cobalt-doped ZnS quantum dots due to a large amount of cobalt doping and this consequently has given rise to a significant distortion resulting in the broadening of the peak in the lattice and thus degrade the crystallinity of the sample, similar studies were reported by Singhal *et al.*^[36]. In comparison with the pure ZnS, certain modifications observed in structural parameters, such as decrement in size, increment in strain and decrement in lattice parameters, illustrate the existence of Co^{2+} ions in the ZnS lattice.

3.2. Morphology studies

3.2.1. SEM analysis

Scanning electron microscopy (SEM) is an effective instrument to analyze surface morphology. Fig. 2 displays the typical SEM micrographs of pure and cobalt-doped ZnS quantum dots. These images have shown that the particles distributions are almost spherical and these quantum dots are agglomerated. The agglomeration and roughness of these particles slightly increase with an increasing dopant concentration. The rough surface is beneficial for gas detection since it can provide more active sites and a high specific surface area required for excellent gas sensing properties.

3.2.2. TEM analysis

The microstructure of pure and cobalt-doped ZnS quantum dots was also examined in detail with the help of TEM. Fig. 3 displays TEM images of pure and cobalt-doped ZnS quantum dots. From these images, uniform size distribution is observed and the particle average size is in the range of 3–6 nm. The crystallite size calculated from XRD is in good correlation with the average crystallite size values obtained from TEM micrographs.

3.3. Chemical analysis using EDX

EDX is a perfect tool to analyze material chemical composition. Fig. 4 displays the EDX spectrum of pure and cobalt-doped ZnS quantum dots existence of Zn, Co and S are confirmed and no additional element traces are observed in the spectrum. This illustrates that high purity Co-doped ZnS quantum dots can be synthesized by the chemical precipitation process. A precise observation of a low-intensity peak for

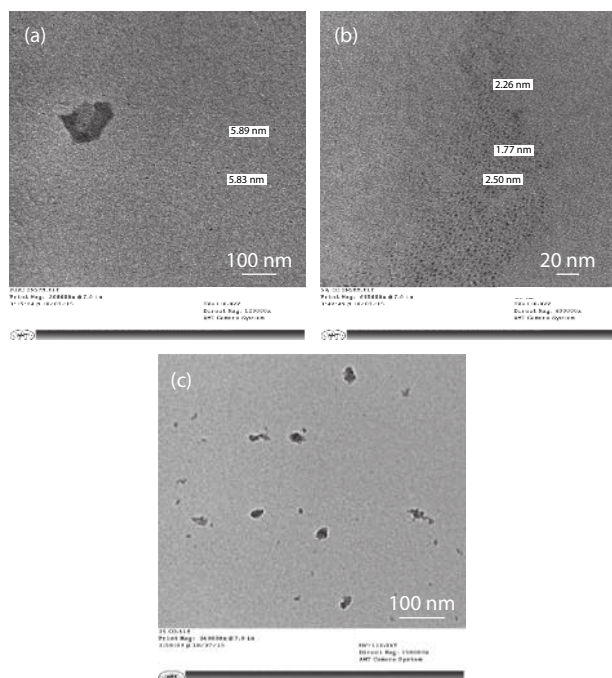


Fig. 3. TEM images of (a) ZnS, (b) 0.05 at.% cobalt-doped ZnS quantum dots (c) 0.25 at.% cobalt-doped ZnS quantum dots

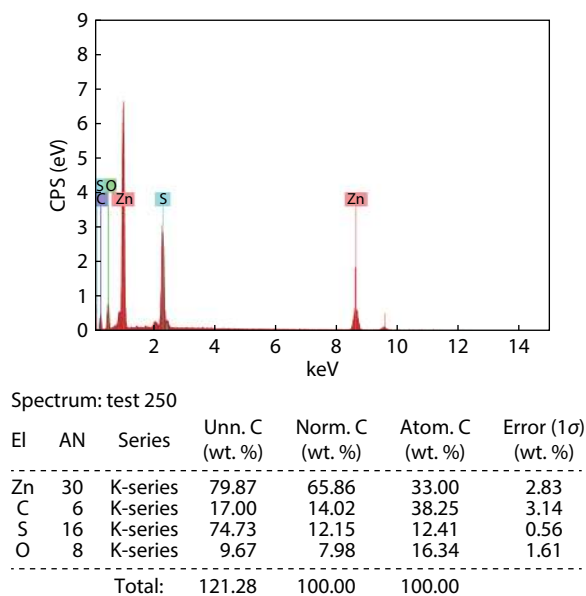
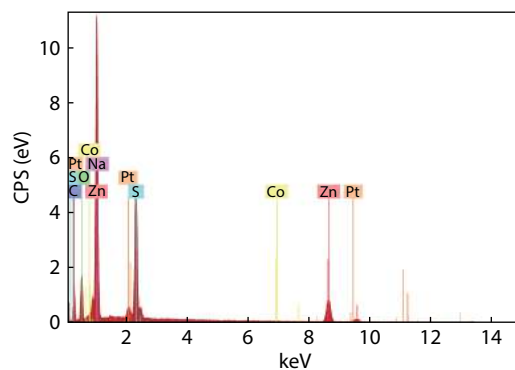


Fig. 4(a). EDX spectra of ZnS quantum dots.

cobalt-doped ZnS shows the proper incorporation of cobalt in the structure.

3.4. Fourier-transform infrared spectroscopy (FTIR)

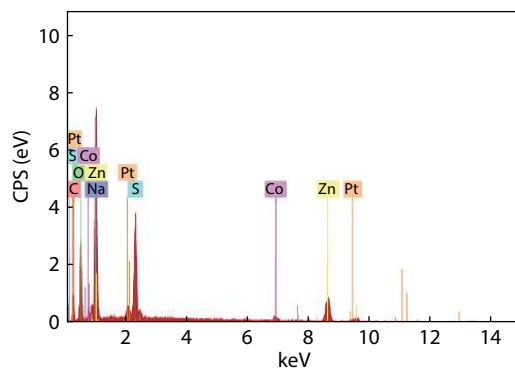
FTIR spectra of pure and cobalt-doped ZnS quantum dots are depicted in Fig. 5. This study will give a qualitative analysis of the adsorbed molecules constrained to the surface of ZnS: Co²⁺ quantum dots. It is clearly observed a broad peak in the range of 3200–3500 cm⁻¹ due to the O–H stretching band due to the absorbed moisture in all the samples. The characteristic peaks appeared at 671.32, 667.54 cm⁻¹ in the prepared samples due to the presence of sulphide in the ZnS samples. These observations are inconsistent with the previously reported work^[37]. The 1399, 1427.51, 1441.52 cm⁻¹ bands are characteristic of hydroxyl groups in the pure ZnS sample. The band at 487.72, 439.21 cm⁻¹ is



Spectrum: test 247

| El | AN | Series | Unn. C (wt. %) | Norm. C (wt. %) | Atom. C (wt. %) | Error (1 σ) (wt. %) |
|--------|----|----------|----------------|-----------------|-----------------|-----------------------------|
| Zn | 30 | K-series | 62.17 | 49.91 | 20.48 | 2.17 |
| C | 6 | K-series | 25.37 | 20.37 | 45.50 | 3.80 |
| S | 16 | K-series | 13.81 | 11.08 | 9.28 | 0.52 |
| O | 8 | K-series | 13.61 | 10.92 | 18.32 | 1.95 |
| Na | 11 | K-series | 6.23 | 5.00 | 5.84 | 0.42 |
| Pt | 78 | K-series | 2.57 | 2.06 | 0.28 | 0.14 |
| Co | 27 | K-series | 0.80 | 0.64 | 0.29 | 0.07 |
| Total: | | | 124.56 | 100.00 | 100.00 | |

Fig. 4(b). EDX spectra of 0.05 at.% cobalt-doped ZnS quantum dots.



| El | AN | Series | Unn. C (wt. %) | Norm. C (wt. %) | Atom. C (wt. %) | Error (1 σ) (wt. %) |
|--------|----|----------|----------------|-----------------|-----------------|-----------------------------|
| Zn | 30 | K-series | 58.97 | 50.47 | 21.80 | 2.27 |
| O | 8 | K-series | 19.36 | 16.57 | 29.24 | 3.07 |
| C | 6 | K-series | 16.53 | 14.15 | 33.27 | 3.40 |
| S | 16 | K-series | 10.11 | 8.65 | 7.62 | 0.41 |
| Na | 11 | K-series | 6.00 | 5.14 | 6.31 | 0.43 |
| Co | 27 | K-series | 3.61 | 3.09 | 1.48 | 0.22 |
| Pt | 78 | M-series | 2.26 | 1.94 | 0.28 | 0.15 |
| Total: | | | 116.84 | 100.00 | 100.00 | |

Fig. 4(c). EDX spectra of 0.25 at.% cobalt-doped ZnS quantum dots.

ascribed to NH₂ symmetric stretching vibration^[38]. The weak bands at frequencies 928.61, 904.91, and 888.54 cm⁻¹ indicate the vibrational modes of interaction between sulfide ions in the crystal.

4. Gas sensing studies

Ammonia is used by fertilizer factories, refrigeration systems and chemical industries. A small leakage in the system can be a critical situation in the industry. Industries using ammonia should have a proper sensor that can immediately alarm to caution when the limit level of ammonia concentration crosses the maximum limit of 50 ppm^[39]. This study successfully synthesized pure ZnS and cobalt-doped ZnS quantum dot sensors to detect a low concentration of ammonia. The response of the gas is calculated by the following equation^[40].

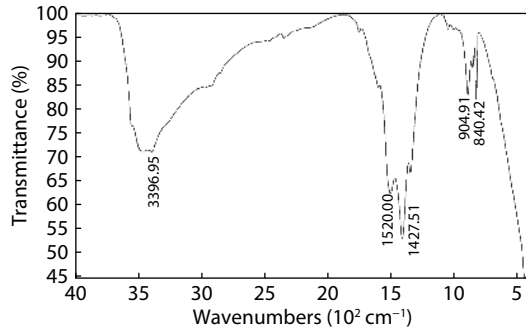


Fig. 5(a). FTIR spectra of ZnS quantum dots.

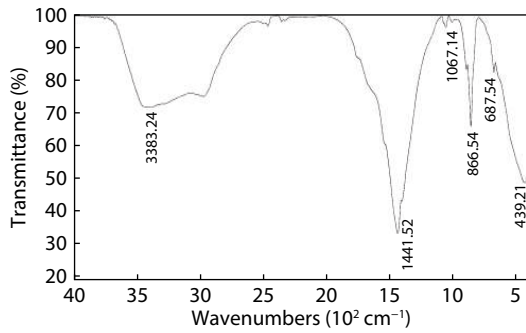


Fig. 5(b). FTIR spectra of 0.05 at.% cobalt-doped ZnS quantum dots.

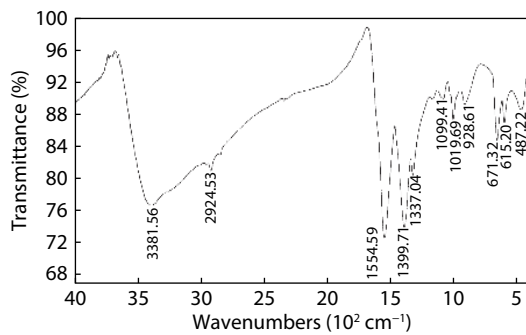


Fig. 5(c). FTIR spectra of 0.25 at.% cobalt-doped ZnS quantum dots.

$$\text{Response\%} = \frac{R_a - R_g}{R_g} \times 100$$

where R_a is the resistance of the sensor in air ambience, and R_g is the resistance in exposed gas.

In present day-to-day life, the optimum temperature is essential to minimize the use of power required for operating practical devices. The ZnS-based quantum dots' response is attributed to the improved surface free energy at an optimum temperature. The increase in native surface states density also leads to the growth of sensors threshold sensitivity, which agrees with the calculated structural parameters. The sensing mechanism in the semiconductor-based materials can be ascribed to the transformation taking place in electrical conductivity/resistance due to the chemical interaction between the surface complexes of O^- , O^{2-} , reactive chemical species (S^{2-}) and gaseous molecules^[41,42]. Adsorption of gas, transfer of charges, and desorption processes are the key factors in this mechanism.

Quantum dots are well thought out in the gas sensors to be a good candidate as the target gas molecules can be easily absorbed as they acquire a high surface area, and by means of Debye length and their grain size is compared.



Fig. 6. Gas sensing setup.

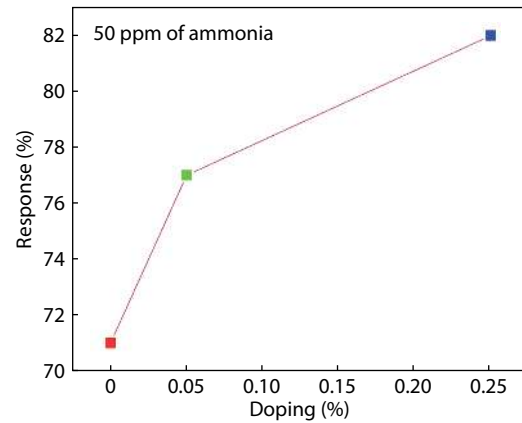
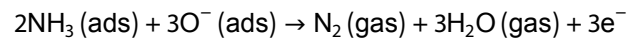


Fig. 7. Response of pure and cobalt-doped ZnS quantum dots towards 50 ppm ammonia.

Thus, when the gas molecules are absorbed, these quantum dots trigger the charge transfer to improve the gas response^[43]. At an optimum temperature of 70°C when the ZnS material is exposed to air, oxygen molecules on the ZnS surface are adsorbed due to the trapping electrons from the conduction band of ZnS, ionized oxygen species such as O^- , O^{2-} are formed relatively^[44, 46]. Then due to the development of the space-charge region, a high resistance state in the air is observed for ZnS. On the surface of the sensing element, the chemisorbed O_2 species interacted with the molecules of ammonia. In the case of ammonia, which is reducing gas, from the baseline, there is a decrease in the surface resistance of the film during the period of interaction with the target gas molecules and the reaction mechanism is shown below:



In cobalt-doped ZnS quantum dots, cobalt nanoparticles activate the target gas by dissociation and subsequent spillover^[47, 48] of dissociation fragments onto the gas sensing material, which causes the target gas response. In the cobalt-doped ZnS gas sensor, cobalt particles increase the molecule to ion conversion rate and the quantity of adsorbed oxygen; as a result, a deeper depletion layer is formed compared to the pure ZnS. When ammonia gas is introduced, the layer would decrease or disappear rapidly, resulting in a dramatic change in the resistance of the semiconductor materials. In a word, cobalt particles increase both the number of oxygen species and the molecule-ion conversion rate, thus significantly enhancing the ammonia sensing properties. Fig. 6 shows the gas sensing equipment in which the sensing measurement is

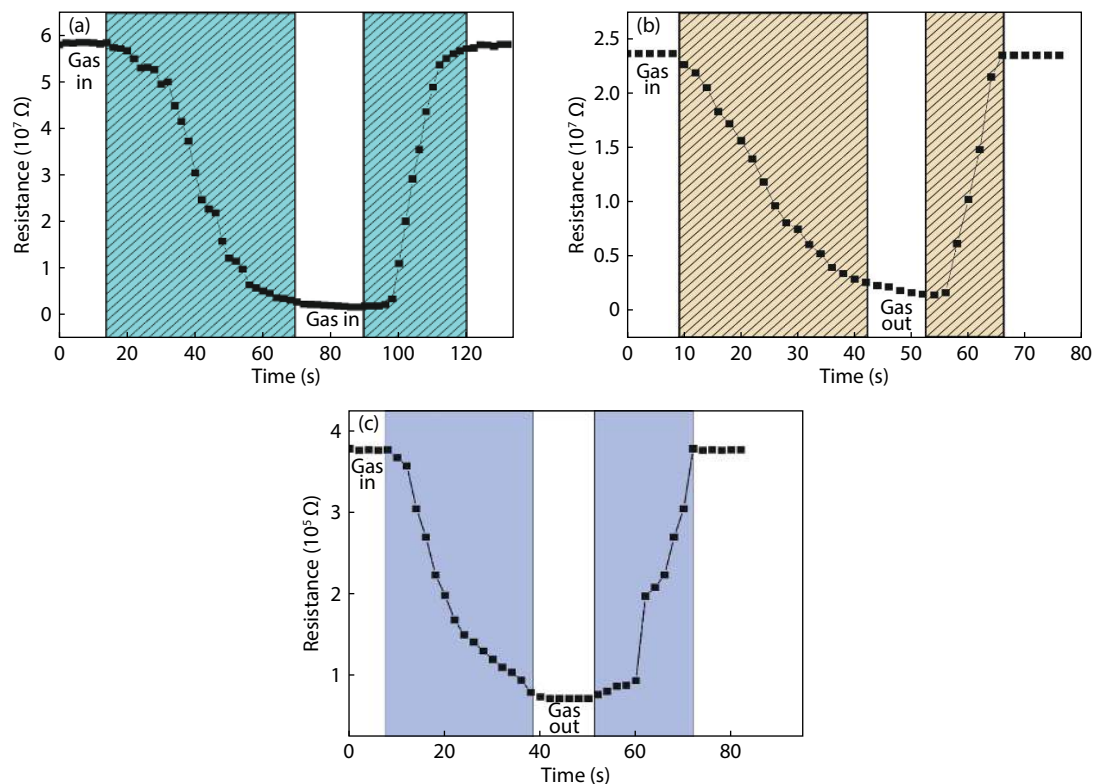


Fig. 8. (Color online) Transient response curves (a) pure ZnS (b) 0.05 at.% of cobalt-doped ZnS quantum dots (c) 0.25 at.% of cobalt-doped ZnS quantum dots.

carried out successfully:

In addition to this, due to the electron-donating reaction, there is an increase in the conductivity of metal oxide for the samples that are doped with transition metal (cobalt). Fig. 7 shows the variation of response % of different sensor elements towards 50 ppm of ammonia gas at an optimum operating temperature of 70 °C. Response at a substantially low temperature is attributed to the increased surface free energy of the nanocrystalline ZnS. It is very clear that the sensor, which is fabricated with 0.25 at.% of cobalt-doped ZnS quantum dot, has shown the maximum response. It might be due to the morphology and the surface state of this sensor being pretty good compared to the other quantum dots.

Fig. 8 shows the transient response curve of pure and cobalt-doped ZnS quantum dots. From the transient curve, response and recovery times are determined. The response time of the sensor elements towards the ammonia gas varies from 48, 35, 26 s and recovery rate as 20, 12, 28 s in the case of pure ZnS, 0.05 at.%, 0.25 at.% cobalt-doped ZnS quantum dots respectively.

The sensor element which is prepared 0.25 at.% of cobalt-doped ZnS exhibits stable response and recovery behaviors. We have also compared the response of this sensor element towards various concentrations of ammonia vapors with available literature. As shown in Table 2, our sensor exhibits better gas sensing properties in terms of response time and ammonia vapour concentration.

5. Conclusions

We have successfully synthesized pure and cobalt-doped ZnS ($Zn_{1-x}Co_xS$, $x = 0.05, 0.25$ at. %) quantum dot sensors with zinc blende structure using a cost-effective co-precipita-

Table 2. Comparison table of gas sensing properties different materials towards ammonia.

| S.No | Material | Concentration (ppm) | Response time (s) | Reference |
|------|---|---------------------|-------------------|--------------|
| 1 | SnO ₂ thin film | 50 | 175 | [49] |
| 2 | CuO-MnO ₂ composite | 100 | 120 | [50] |
| 3 | NiO nanowire | 50 | 36 | [51] |
| 4 | WS ₂ -TiO ₂ nanohybrids | 200 | 250 | [52] |
| 5 | Ni-ZnO | 750 | 46 | [53] |
| 6 | TiO ₂ modified ZnO thick film | 100 | - | [54] |
| 7 | Cobalt doped ZnS quantum dot | 50 | 26 | Present work |

tion method. The structural studies from XRD reveal that the formation of well-crystalline quantum dots with a crystallite size less than 5 nm. EDX analysis revealed Zn and S elements in the pure sample Zn, S, Co, in cobalt-doped samples. SEM images reveal the smaller grain size and spherical shape of cobalt-doped samples, while TEM confirms the particle size is in the range of 6 nm. The morphology and surface state is increased with increasing cobalt concentration. Spectroscopic investigation using FTIR analysis shows the changes observed at different vibrational modes. The gas sensing characterization of pure and cobalt-doped ZnS quantum dots were investigated towards 50 ppm of ammonia. Among these samples, 0.25 at% cobalt doped ZnS quantum dots were shown the maximum response of 82% towards 50 ppm of ammonia vapors at an operating temperature of 70 °C with a response time of 26 s and recovery time of 28 s. We firmly believe that this sensor can be suitable to detect the low concentration of

ammonia vapours.

References

- [1] Fan G Y, Wang C Y, Fang J Y. Solution-based synthesis of III-V quantum dots and their applications in gas sensing and bio-imaging. *Nano Today*, 2014, 9, 69
- [2] Xiang D H, Zhu Y B, He Z J, et al. A simple one-step synthesis of ZnS nanoparticles via salt-alkali-composited-mediated method and investigation on their comparative photocatalytic activity. *Mater Res Bull*, 2013, 48, 188
- [3] Fang X S, Zhai T Y, Gautam U K, et al. ZnS nanostructures: From synthesis to applications. *Prog Mater Sci*, 2011, 56, 175
- [4] Liu H, Hu L F, Watanabe K, et al. Cathodoluminescence modulation of ZnS nanostructures by morphology, doping, and temperature. *Adv Funct Mater*, 2013, 23, 3701
- [5] Xu X J, Li S Y, Chen J X, et al. Design principles and material engineering of ZnS for optoelectronic devices and catalysis. *Adv Funct Mater*, 2018, 28, 1802029
- [6] Fang, Gautam U K, Bando Y, et al. Multiangular branched ZnS nanostructures with needle-shaped tips: potential luminescent and field-emitter nanomaterial. *J Phys Chem C*, 2008, 112, 4735
- [7] Fang X S, Bando Y, Liao M Y, et al. Single-crystalline ZnS nanobelts as ultraviolet-light sensors. *Adv Mater*, 2009, 21, 2034
- [8] Jadraque M, Evtushenko A B, Ávila-Brandé D, et al. Co-doped ZnS clusters and nanostructures produced by pulsed laser ablation. *J Phys Chem C*, 2013, 117, 5416
- [9] Poornaprakash B, Amaranatha Reddy D, Murali G, et al. Composition dependent room temperature ferromagnetism and PL intensity of cobalt doped ZnS nanoparticles. *J Alloys Compd*, 2013, 577, 79
- [10] Fan G Y, Wang C Y, Fang J Y. Solution-based synthesis of III-V quantum dots and their applications in gas sensing and bio-imaging. *Nano Today*, 2014, 9, 69
- [11] Xiang D H, Zhu Y B, He Z J, et al. A simple one-step synthesis of ZnS nanoparticles via salt-alkali-composited-mediated method and investigation on their comparative photocatalytic activity. *Mater Res Bull*, 2013, 48, 188
- [12] Fang X S, Zhai T Y, Gautam U K, et al. ZnS nanostructures: From synthesis to applications. *Prog Mater Sci*, 2011, 56, 175
- [13] Liu H, Hu L F, Watanabe K, et al. Cathodoluminescence modulation of ZnS nanostructures by morphology, doping, and temperature. *Adv Funct Mater*, 2013, 23, 3701
- [14] Xu X J, Li S Y, Chen J X, et al. Design principles and material engineering of ZnS for optoelectronic devices and catalysis. *Adv Funct Mater*, 2018, 28, 1802029
- [15] Fang, Gautam U K, Bando Y, et al. Multiangular branched ZnS nanostructures with needle-shaped tips: potential luminescent and field-emitter nanomaterial. *J Phys Chem C*, 2008, 112, 4735
- [16] Fang X S, Bando Y, Liao M Y, et al. Single-crystalline ZnS nanobelts as ultraviolet-light sensors. *Adv Mater*, 2009, 21, 2034
- [17] Jadraque M, Evtushenko A B, Ávila-Brandé D, et al. Co-doped ZnS clusters and nanostructures produced by pulsed laser ablation. *J Phys Chem C*, 2013, 117, 5416
- [18] Poornaprakash B, Amaranatha Reddy D, Murali G, et al. Composition dependent room temperature ferromagnetism and PL intensity of cobalt doped ZnS nanoparticles. *J Alloys Compd*, 2013, 577, 79
- [19] Fang W J, Liu Y S, Guo B Z, et al. Room temperature ferromagnetism and cooling effect in dilute Co-doped ZnS nanoparticles with zinc blende structure. *J Alloys Compd*, 2014, 584, 240
- [20] Tang L J, Huang G F, Tian Y, et al. Efficient ultraviolet emission of ZnS nanospheres: Co doping enhancement. *Mater Lett*, 2013, 100, 237
- [21] Akhtar M S, Malik M A, Riaz S, et al. Optimising conditions for the growth of nanocrystalline ZnS thin films from acidic chemical baths. *Mater Sci Semicond Process*, 2015, 30, 292
- [22] Hou Q T, Chen K, Zhang H G, et al. Magnetic properties of co doped ZnS diluted magnetic semiconductor. *J Phys: Conf Ser*, 2013, 430, 012076
- [23] Zhang L, Qin D Z, Yang G R, et al. The investigation on synthesis and optical properties of ZnS: Co nanocrystals by using hydrothermal method. *Chalcog Lett*, 2012, 9, 93
- [24] Liu L Y, Yang L, Pu Y T, et al. Optical properties of water-soluble Co²⁺: ZnS semiconductor nanocrystals synthesized by a hydrothermal process. *Mater Lett*, 2012, 66, 121
- [25] Chen X B, Yang N, Liu X F, et al. Structure dependent photoluminescence and magnetic properties of Co: ZnS nanostructures. *Phys Scr*, 2013, 88, 035703
- [26] Ehsan M A, Peiris T A N, Wijayantha K G U, et al. Surface morphological and photoelectrochemical studies of ZnS thin films developed from single source precursors by aerosol assisted chemical vapour deposition. *Thin Solid Films*, 2013, 540, 1
- [27] Sullivan H, Parish J D, Thongchai P, et al. Aerosol-assisted chemical vapor deposition of ZnS from thioureide single source precursors. *Inorg Chem*, 2019, 58, 2784
- [28] Parkin I P, Price L S, Hibbert T G, et al. The first single source deposition of tin sulfide coatings on glass: Aerosol-assisted chemical vapour deposition using [Sn(SCH₂CH₂S)₂]. *J Mater Chem*, 2001, 11, 1486
- [29] Memon A A, Afzaal M, Malik M A, et al. The N-alkyldithiocarbamate complexes [M(S₂CNHR)₂] (M = Cd(II) Zn(II); R = C₂H₅, C₄H₉, C₆H₁₃, C₁₂H₂₅); their synthesis, thermal decomposition and use to prepare of nanoparticles and nanorods of CdS. *Dalton Trans*, 2006, 4499
- [30] Istaş J R, de Borger R, de Temmerman L, et al. Effect of ammonia on the acidification of the environment. European Communities Report No. EUR 11857 EN, 1988.
- [31] Timmer B, Olthuis W, van den Berg A. Ammonia sensors and their applications—a review. *Sens Actuat B*, 2005, 107, 666
- [32] Binks D J, Bant S P, West D P, et al. CdSe/CdS core/shell quantum dots as sensitizer of a photorefractive polymer composite. *J Mod Opt*, 2003, 50, 299
- [33] Nguyen C Q, Adeogun A, Afzaal M, et al. Metal complexes of selenophosphinates from reactions with (R₂PSe)₂Se: [M(R₂PSe)_n] (M = ZnII, CdII, PbII, InIII, GaIII, CuI, BiIII, NiII; R = iPr, Ph) and [MoV₂O₂Se₂(Se₂PiPr₂)₂]. *Chem Commun*, 2006, 2182
- [34] Derbali A, Saidi H, Attaf A, et al. Solution flow rate influence on ZnS thin films properties grown by ultrasonic spray for optoelectronic application. *J Semicond*, 2018, 39, 093001
- [35] Panneerselvam A, Nguyen C Q, Malik M A, et al. The CVD of silver selenide films from dichalcogenophosphinato and imidodichalcogenodiphosphinatosilver(I) single-source precursors. *J Mater Chem*, 2009, 19, 419
- [36] Singhal S, Chawla A K, Gupta H O, et al. Influence of cobalt doping on the physical properties of Zn_{0.9}Cd_{0.1}S nanoparticles. *Nanoscale Res Lett*, 2009, 5, 323
- [37] Salem J K, Hammad T M, Kuhn S, et al. Structural and optical properties of Co-doped ZnS nanoparticles synthesized by a capping agent. *J Mater Sci: Mater Electron*, 2014, 25, 2177
- [38] Poornaprakash B, Amaranatha Reddy D, Murali G, et al. Composition dependent room temperature ferromagnetism and PL intensity of cobalt doped ZnS nanoparticles. *J Alloys Compd*, 2013, 577, 79
- [39] Sarte P M, Cowley R A, Rodriguez E E, et al. Disentangling orbital and spin exchange interactions for Co²⁺ on a rocksalt lattice. *Phys Rev B*, 2018, 98, 024415
- [40] Yang A M, Sheng Y H, Farid M A, et al. Copper doped EuMnO₃: Synthesis, structure and magnetic properties. *RSC Adv*, 2016, 6, 13928
- [41] Nagaraju P, Vijayakumar Y, Ramana Reddy M V. Room-temperature BTEX sensing characterization of nanostructured ZnO thin

- films. *J Asian Ceram Soc*, 2019, 7, 141
- [42] Abbas N K, Al-Rasoul K T, Shanan Z J. New method of preparation ZnS nano size at low pH. *Int J Electrochem Sci*, 2013, 8, 3049
- [43] Kumar S, Mandal P, Singh A, et al. Magnetization properties of Co incorporated ZnS nanocrystals synthesized at low temperature via chemical route. *J Alloys Compd*, 2020, 830, 154640
- [44] Nagaraju P, Vijayakumar Y, Phase D M, et al. Microstructural, optical and gas sensing characterization of laser ablated nanostructured ceria thin films. *J Mater Sci: Mater Electron*, 2016, 27, 651
- [45] Singhal S, Chawla A K, Gupta H O, et al. Influence of cobalt doping on the physical properties of $Zn_{0.9}Cd_{0.1}S$ nanoparticles. *Nanoscale Res Lett*, 2009, 5, 323
- [46] Ghosh G, Kanti Naskar M, Patra A, et al. Synthesis and characterization of PVP-encapsulated ZnS nanoparticles. *Opt Mater*, 2006, 28, 1047
- [47] Rema Devi B S, Raveendran R, Vaidyan A V. Synthesis and characterization of Mn^{2+} -doped ZnS nanoparticles. *Pramana*, 2007, 68, 679
- [48] Timmer B, Olthuis W, van den Berg A. Ammonia sensors and their applications—a review. *Sens Actuat B*, 2005, 107, 666
- [49] Manjunath G, Vardhan R V, Praveen L L, et al. Room-temperature detection of ammonia and formaldehyde gases by $La_xBa_{1-x}SnO_{3-\delta}$ ($x = 0$ and 0.05) screen printed sensors: Effect of ceria and ruthenate sensitization. *Appl Phys A*, 2021, 127, 1
- [50] Godavarti U, Mote V D, Reddy M V R, et al. Precipitated cobalt doped ZnO nanoparticles with enhanced low temperature xylene sensing properties. *Phys B*, 2019, 553, 151
- [51] Bhat P, K N K S, Nagaraju P. Synthesis and characterization of ZnO-MWCNT nanocomposites for 1-butanol sensing application at room temperature. *Phys B*, 2019, 570, 139
- [52] Liu Y L, Wang L L, Wang H R, et al. Highly sensitive and selective ammonia gas sensors based on PbS quantum dots/TiO₂ nanotube arrays at room temperature. *Sens Actuat B*, 2016, 236, 529
- [53] Li Z P, Zhao Q Q, Fan W L, et al. Porous SnO₂ nanospheres as sensitive gas sensors for volatile organic compounds detection. *Nanoscale*, 2011, 3, 1646
- [54] Chen Z G, Zou J, Liu G, et al. Silicon-induced oriented ZnS nanobelts for hydrogen sensitivity. *Nanotechnology*, 2008, 19, 055710
- [55] Liu Y G, Feng P, Xue X Y, et al. Room-temperature oxygen sensitivity of ZnS nanobelts. *Appl Phys Lett*, 2007, 90, 042109
- [56] Liu X W, Wang F Y, Zhen F, et al. *In situ* growth of Au nanoparticles on the surfaces of Cu₂O nanocubes for chemical sensors with enhanced performance. *RSC Adv*, 2012, 2, 7647
- [57] Batzill M, Diebold U. Surface studies of gas sensing metal oxides. *Phys Chem Chem Phys*, 2007, 9, 2307
- [58] Wang X F, Xie Z, Huang H T, et al. Gas sensors, thermistor and photodetector based on ZnS nanowires. *J Mater Chem*, 2012, 22, 6845
- [59] Park S, An S, Ko H, et al. Synthesis, structure, and UV-enhanced gas sensing properties of Au-functionalized ZnS nanowires. *Sens Actuat B*, 2013, 188, 1270
- [60] Hussain S, Liu T M, Javed M S, et al. Highly reactive 0D ZnS nanospheres and nanoparticles for formaldehyde gas-sensing properties. *Sens Actuat B*, 2017, 239, 1243
- [61] Zhang L P, Dong R, Zhu Z Y, et al. Au nanoparticles decorated ZnS hollow spheres for highly improved gas sensor performances. *Sens Actuat B*, 2017, 245, 112
- [62] Mani G K, Rayappan J B B. Selective detection of ammonia using spray pyrolysis deposited pure and nickel doped ZnO thin films. *Appl Surf Sci*, 2014, 311, 405
- [63] Kalyamwar V S. TiO₂ modified ZnO thick film resistors as ammonia gas sensors. *Adv Mater Lett*, 2013, 4, 895



Uma Devi Godavarti is currently working as an Associate Professor in CMR Technical campus, Hyderabad, Telangana, India. She did her Post-graduate studies in Physics from Osmania University, Telangana. She received her PhD in 2019 from Gitam Deemed to be University, Visakhapatnam. She is also a life member of Indian society for technical education. She published nine research articles in peer-reviewed journals. Her research expertise is in nanotechnology, material synthesis and its applications particularly in gas sensing mechanism.



P. Nagaraju is presently working as Professor of Physics, CMR Technical Campus, Hyderabad, Telangana State, India. He completed his Post graduation from Kakatiya University, Warangal, in 2004 and received PhD in the year 2015 from Osmania University, Hyderabad, Telangana State. He is also a life member of the Indian Science Congress, Indian Society for Technical Education, Sensor Society of India and Magnetic Society of India. He has published more than 35 research papers in peer-reviewed journals. He is also an active reviewer for several reputed journals. He has received out-standing reviewer award from the *Sensors & Actuators B*, which is a pioneer journal in the field of sensors. He is a recipient of an Early Career Research Award from the Department of Science & Technology, Science and Engineering Research Board, Government of India.